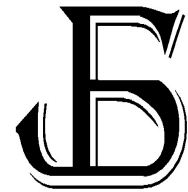# Robust fractional order sliding mode control for solar based DC-AC inverter

Shaik Silar Saheb [iD]

Gayatri Vidya Parishad College of Engineering, (Autonomous), Madhurawada Andhra Pradesh, India,
silar283@gmailcom

Satish Kumar Gudey [iD]

Gayatri Vidya Parishad College of Engineering, (Autonomous), MadhurawadaAndhra Pradesh, India,
satishgudey13@gmail.com

Abstract: Fractional order sliding mode control (FOSMC) strategy for a solar based DC-AC inverter is presented in this work. First FOSMC is implemented to voltage source inverter with a fixed DC input voltage of 400V to drive a load of 2.3 kW at a power factor of 0.8 lag. Here the load voltage and current through capacitor as state variables and a linear sliding surface are considered. FOSMC using Gao's reaching law is derived for inverter circuit. FOSMC is implemented at load bus to control output voltage of inverter with linear and nonlinear loads to desired values. FOSMC controls the output voltage with good voltage regulation, less steady state error of 1.32 %, settling time of 0.15 ms, good dynamic response, and convergence to origin with less chattering compared to classical SMC. FOSMC based solar based VSI is presented. The maximum power from PV array is extracted using P&O MPPT algorithm. A boost converter is used to step up input voltage of 200 V to 400 V. P-V and I-V characteristics are obtained for a typical solar cell of 2.5 kW FOSMC requires less control efforts to obtain a pure sinusoidal output voltage waveform of 230 V (rms) with output voltage THD of 0.135% well within IEEE standards. PSCAD/EMTDC v4.6 is used for simulation work

Keywords: *Fractional order sliding mode control, Chattering, Dynamic response, Convergence, Solar (PV) system.*

Cite this paper as:	Saheb, S.S.&Gudey, S.K.,Robust fractional order sliding mode control for solar based DC-AC inverter. *Journal of Energy Systems* 2020, *4*(4), 161-178, DOI: 10.30521/jes.737264

1. INTRODUCTION

In India, many remote locations and areas are blessed with abundant sun energy. Therefore the photovoltaic panels, DC-DC converters, DC-AC inverters can be integrated to generate and distribute power to a distributed energy resource system (DES) which can supply power to these remote locations. It reduces the burden on the grid. Here the voltage source inverter (VSI) plays an important role in the conversion. A VSI develops a pure sinusoidal waveform of desired magnitude and phase difference for all practical applications in the industry. It needs a good controller. The controller can be a variable frequency one like a hysteresis controller or a fixed frequency controller like a PWM. All loads require a stable AC voltage. It's always challenging to develop new control strategies for a VSI to such industrial loads [1].

There are many inverter control methods like the hysteresis current control, model predictive control, variable structure control like SMC techniques. These techniques have merits and demerits in producing a pure sinusoidal output voltage waveforms. Most of them are well developed and available in the literature [1-2]. All these controllers should possess black start capability [2] good stability and fast transient responses. Also they should be insensitive towards parametric variations in the system. In total the response should be robust and dynamic in producing a pure sinusoidal output voltage waveform.

Sliding Mode Control (SMC) is a robust controller which guarantees excellent tracking during systems exposure to parametric variations and external perturbances [3]. Designing a novel sliding surface that suits the system for closed loop operation is the first step in SMC. Next is to design a suitable control law such that the desired state variable trajectories follow and slide on the sliding surface to the origin. The system is then said to be stable [4].

The merits of SMC are its high precision and simple to implement. Chattering due to high frequency oscillations nearby sliding surface due to defined control law which is always discontinuous in SMC. Chattering affects the system in terms of decreasing the control accuracy, more heat losses in electrical circuits and lessens the life of mechanical parts. Using higher order SMC like twisting, super twisting, enhanced exponential reaching law based SMC, terminal SMC etc. the chattering can be reduced [5-8] to realize excellent control accuracy. These controllers based on SMC are developed by using integer order calculus. A fractional order SMC (FOSMC) involves fractional order integrator and differentiator giving better performance when it is utilized for closed loop control of fractional order systems than the conventional SMC. It provides additional control parameters for obtaining optimum dynamic response. Since fractional calculus is a well-developed area of mathematics, one can utilize it to design FOSMC [9]. Presently, FOSMC is used in all engineering applications in the fields of feedback control, systems theory, robotics and signals processing. It is used in wind energy conversion systems, PV systems, lighting control systems sensorless vector controlled induction motors etc., in the field of electrical engineering [2].

Designing the sliding surface is based on Fractional calculus theory in FOSMC. Robustness and accuracy improvement is provided by the fractional order term which gives an extra level of freedom for SMC. The characteristics of fractional calculus in FOSMC adds towards reduction in high frequency oscillations in the system. From the robust control view, a FOSMC is meritorious owing to its extra design parameters i.e. controllable non-integer differentiator / integrator fractional order [10-14]. Fig. 1 shows the generalized block diagram for FOSMC. Sliding surface S is obtained when actual variable X_{act} is compared with the desired variable X_{ref} [15]. This sliding surface is processed through the FOSMC block to produce the gating pulses to the VSI circuit. The output voltage waveform is well regulated in a VSI.
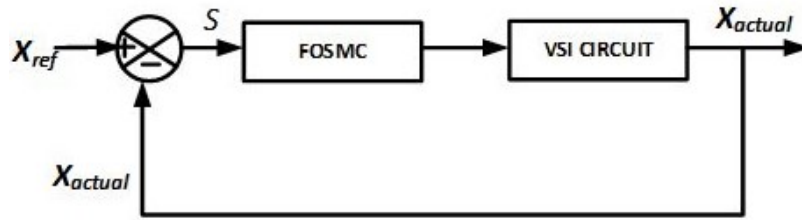
Figure1. FOSMC generalized block diagram.

Nowadays for meeting the increasing load demand, the effective integration of renewable energy sources like Photovoltaic (PV) is very much necessary. PV systems are used to convert solar energy into electrical energy. A PV cell has a highly nonlinear characteristic and the output voltage depends on ambient temperature and solar irradiation. Therefore the loads cannot be directly connected to the solar PV panels. A maximum power point tracking (MPPT) algorithm is required to optimize the extraction of DC power from the PV panels and also to increase its efficiency. Therefore many MPPT algorithms have been developed in the literature such as Perturb and Observe, Incremental Conductance, Hill Climbing etc. to extract maximum energy from the PV panel using a power electronic converter circuit [4]. Most of these algorithms are 90% to 95% efficient in the energy conversion.

The PV system comprises of an array of solar panels known as a PV array, a DC-DC boost converter and a VSI for standalone and grid interface applications [15]. A boost converter converts the low voltage obtained from a PV array using MPPT algorithm with suitable controller to a required high voltage and then fed to a VSI to generate a desired output AC voltage waveform. More details about PV systems and MPPT algorithm are presented in the later part of the work.

In Ref. [16], FOSMC based on PI and PID controllers are proposed for a DC-DC Buck converter for robustness and less sensitivity towards perturbations is presented. The work presented here is the application of FOSMC for a VSI circuit for robustness. The state space model is derived in a classical way to find the control input equation using a PID sliding surface. In [17] a Fractional order Terminal Sliding Mode controller (FTSMC) is proposed for a DC-DC buck converter for finite convergence of the output voltage and also for good dynamic response during load changes. With the basic application of FOSMC presented here, it can be extended to a FTSMC for a VSI circuit for grid as well as standalone operation as a future scope. Similarly, Adaptive FTSMC proposed in [18] for a DC-DC buck converter can very well be extended for DC-AC inverter for smaller steady state error and finite convergence. In Ref. [19] the authors presented a FOSMC based on PI controller, which provides robustness, noise attenuation and reduced overshoot with fast dynamic response of 3ms. This work uses a PID sliding surface and provides good dynamic response in 0.15 ms. In [20] a FOSM current controller is proposed for a QZSI for PV grid connected inverter in which the inductor current is taken as a state variable and achieved higher robustness and stability for input side disturbances. In this work, a Solar based DC-AC inverter with FOSMC voltage controller is simulated with voltage cross the capacitor and the current through the capacitor as state variables to regulate the output voltage and to reduce chattering present in a classical SMC during standalone operation. In Ref. [21], a chattering free response is presented with FOSMC for a three phase DC-AC inverter during grid operation for active and reactive power control. Compared to this work, the paper presents phase plane portraits for chattering observation for FOSMC when VSI is connected to different loads.

The main contributions of the work are as follows: (i) FOSMC is presented for a single phase VSI working in standalone mode of operation. The state space model of VSI is derived and the control input equation is obtained for FOSMC based on PID sliding surface, (ii) Performance parameters such as dynamic response, steady state error, settling time, THD, chattering through phase plane portraits are presented. (iii) A solar based DC-AC inverter with FOSMC is presented as an application with different loads along with the performance characteristics using P&O MPPT algorithm, (iv) A

comparison with the classical SMC is presented to highlight the features of FOSMC of less settling time, steady state error and chattering.

The work presents a model of the VSI and FOSMC control development in Section 1 followed by the modeling of VSI and FOSMC development in Section 2. Section 3 presents the implementation of FOSMC with simulation results of a single phase VSI feeding different loads in Section 4. The dynamic and the steady state responses are realized. Section 5 presents the solar based DC-AC inverter with FOSMC. Simulation results are presented in PSCAD v4.6 in Section 6. The conclusions stand in the last section.

2. MODEL OF VSI AND FOSMC CONTROL DEVELOPMENT
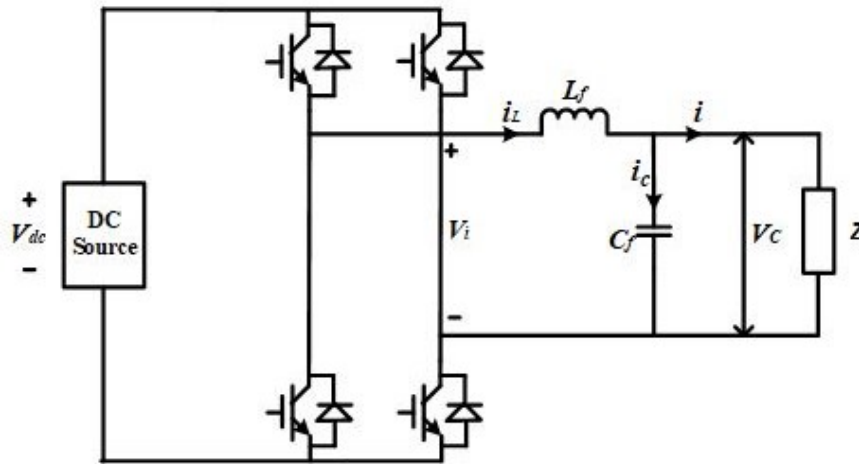
Figure 2. Power circuit of a 1-Phase VSI.

The state space equations are given by Eq. (1) and Eq. (2)

$$\dot{x} = Ax + Bu \tag{1}$$

$$y = Cx \tag{2}$$

Where state variable is x, $\dot{x}$ is derivative of the state variable, u is the control input and the output variable is y, state transition matrix is represented by A, B is the input matrix. The mathematical model of VSI circuit is derived using i_L and v_c as state variables and is given by Eq. (3)

$$\begin{bmatrix} \dot{i}_L \\ \dot{v}_c \end{bmatrix} = \begin{bmatrix} 0 & \dfrac{-1}{L} \\ \dfrac{1}{C} & \dfrac{-1}{Z.C} \end{bmatrix} \begin{bmatrix} i_L \\ v_c \end{bmatrix} + \begin{bmatrix} \dfrac{V_{DC}}{L} \\ 0 \end{bmatrix} u \tag{3}$$

In this paper, the sliding surface of FOSMC for VSI is considered as Eq. (4):

$$S = K_p e + K_i D^{-\lambda} + K_d D^{\mu} e \tag{4}$$

Where μ and λ are fractional order derivative and integral and e is the error voltage given by $e = v_r - v_c$ v_r is the required voltage and v_c is the sensed output voltage of a VSI circuit. Taking the first derivative, we have Eqs. (5,6):

$$S^1 = K_p e^1 + K_i D^{-\lambda} e + K_d D^\mu (v_r^1 - v_c^1) \tag{5}$$

$$S^1 = K_p e^1 + K_i D^{1-\lambda} e + K_d D^{\mu-1} (v_r^{11} - v_c^{11}) \tag{6}$$

Using Gao's Reaching Law [11, 12];

$$S^1 = -K \operatorname{sgn}(S) \tag{7}$$

By equating both the Eq. (6) and Eq. (7), ,one gets

$$-K \operatorname{sgn}(S) = K_p e^1 + K_i D^{1-\lambda} e + K_d D^{\mu-1} (v_r^{11} - v_c^{11}) \tag{8}$$

$$K_d D^{\mu-1} (v_r^{11} - v_c^{11}) = -K_p (v_r^1 - v_c^1) - K_i D^{1-\lambda} (v_r - v_c) - K \operatorname{sgn}(S) \tag{9}$$

Now, using Eq. (3), we obtain the second derivative of output voltage as Eq. (11):

$$v_c^1 = \frac{i_L}{C} - \frac{1}{ZC} v_c \tag{10}$$

$$v_c^{11} = \frac{-1}{LC} v_c + \frac{V_{DC}}{LC} u - \frac{1}{ZC} v_c^1 \tag{11}$$

Simplifying and rearranging the terms the control input u is obtained as Eq. (13):

$$D^{\mu-1} u = \frac{-K_p LC}{K_d V_{DC}} [v_r^1 - \frac{i_L}{C} - \frac{1}{ZC} v_c] + D^{\mu-1} \frac{v_c}{V_{DC}} + \frac{L}{V_{DC} Z} D^{\mu-1} v_c^1 - \frac{K_i LC}{K_d V_{DC}} D^{1-\lambda} [v_r - v_c] - \frac{K_i LC}{K_d V_{DC}} K \operatorname{sgn}(S) - \frac{LC}{V_{DC}} D^{\mu-1} v_r^1 \tag{12}$$

$$u = v_c [\frac{1}{V_{DC}}] + v_c^1 [\frac{LC}{V_{DC} ZC} - \frac{K_p LC}{K_d V_{DC}} + \frac{K_i LC}{K_d V_{DC}} D^{1-\mu-\lambda}] + v_r^1 [\frac{-K_p L}{K_d V_{DC}}] + v_r^{11} [\frac{-LC}{V_{DC}}] + \frac{K_i LC}{K_d V_{DC}} D^{1-\mu} K \operatorname{sgn}(S) \tag{13}$$

The FOSMC control equation is given by Eq. (13) based on a PID sliding surface [21-23].

3. FOSMC IMPLEMENTATION

A first order sliding surface s is derived using the current through the capacitor i_c and voltage across the capacitor v_c as state variables. In Fig. 3, S passes through a FOSMC block and S_{FOSMC} is obtained as Eq. (4). To generate the switching pulses, PWM (the obtained output signal is compared with a carrier wave) [24-26] is used comprising of a triangular waveform operating at 10 kHz switching frequency.
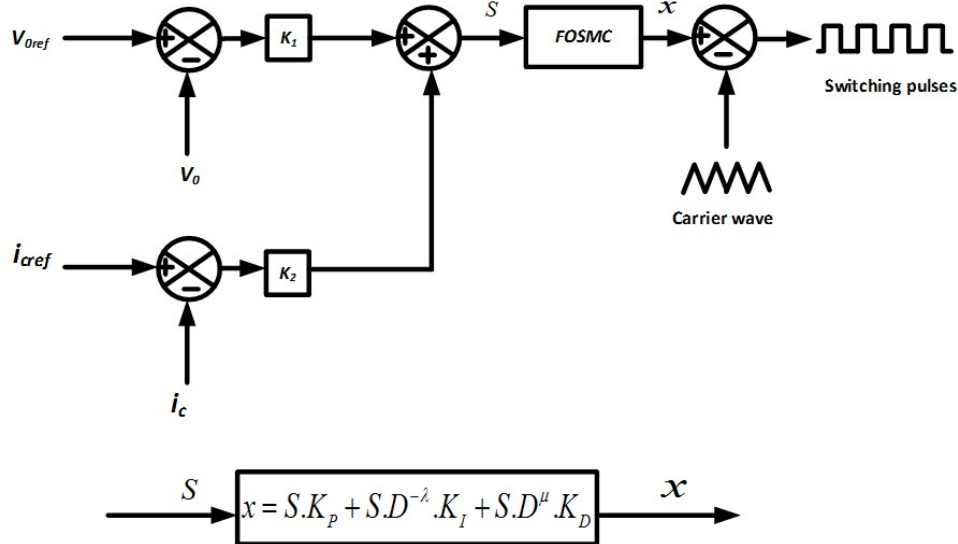
$$x = S.K_P + S.D^{-\lambda}.K_I + S.D^{\mu}.K_D$$

Figure 3. Proposed FOSMC control scheme.

$$V_{0_{ref}} = V_{C_{ref}} = V_m \sin \omega t \tag{14}$$

$$i_{c_{ref}} = c.\frac{dv_{c_{ref}}}{dt} = c.\frac{dv_{0_{ref}}}{dt} \tag{15}$$

The pulses so obtained are used to turn on the IGBT switches and hence the load gets connected to the source and the power transfer takes place. The reference capacitor voltage and reference capacitor current values are obtained as Eqs. (14,15). *S* tends to zero and derivative of *S* being zero are the two conditions to be satisfied for the existence of FOSMC [1]. Eq. (16) defines the control law as;

$$u = \begin{cases} +1 \, for \, S > V_{tri} \\ -1 \, for \, S < V_{tri} \end{cases} \tag{16}$$

V_{tri} is the repetitive signal with a suitable switching frequency. Lyapunov function defines the stability using the Eq. (17) [1].

$$V(t) = \frac{1}{2}S^2(t) + \frac{1}{2}\dot{S}^2(t) \tag{17}$$

4. SIMULATION RESULTS

A VSI circuit with an *LC* filter on the output side is operated using the proposed FOSMC. The circuit works at a constant switching frequency of 10 kHz. For a given desired sinusoidal output voltage of $v_{oref} = 230 \sin (\omega t)$ simulation results are presented for different types of loads. Those are linear and non-linear loads. Table 1 refers to the configuration parameters used for the work. *u,* the control input *u* is obtained from Eq. (13) and is given by Eq. (18):

$$u = v_c^1 \left[6.66 \times 10^{-8} \right] + v_{ref}^1 \left[2.81 \times 10^{-3} \right] D^{-0.5} + v_{ref}^{11} \left[-6.19 \times 10^{-10} \right] + \\ 6.197 \times k \, \text{sgn}(s) D^{0.5} + 0.909 \tag{18}$$

Table 1 Configuration Variables

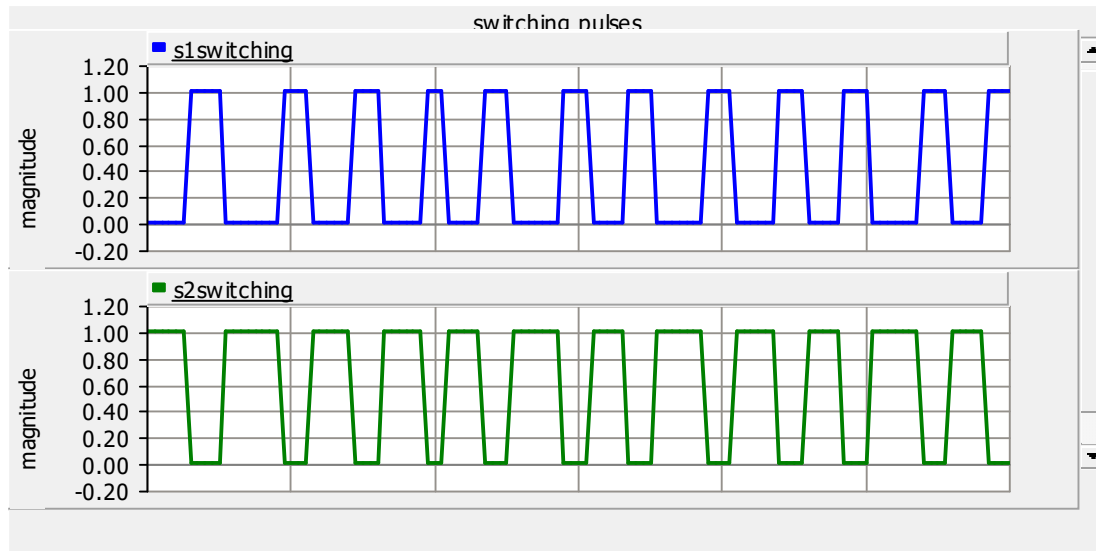| Variables	Value
Input voltage V_{dc}	355 V
Power frequency f	50 Hz
Inductance L_f	1 mH
Capacitance C_f	220 μF
Load Z,Non Linear Load –Diode bridge with series RL on the dc side	2.3 kW, 0.8 pf lag
Switching frequency f_s	10 kHz
Tuning parameters k_1, k_2	100, 0.1
PID k_p, k_i, k_d	100,0.01,0.1
Fractional order differentiator and integrator variables μ, λ	1,0.5

Figure 4. Complementary IGBT Gating Pulses.

Fig. 4 represents the switching pulses obtained by using FOSMC. These gating pulses are given to the IGBT switches which connect the load and the source. Fig. 5 represents the tracking of the desired 230 V rms output voltage with the corresponding sensed output voltage. The FOSMC is able to track the desired reference with 7.7 ms settling time and steady state error of 1.32 %. Fractional order sliding surface with a magnitude of 1V (peak) is shown in Fig. 6. The load current and voltage in phase for a resistive load as shown in Fig. 7. Fig. 8 shows the dynamic response plot obtained when the load is suddenly reduced to half from 0.1 s to 0.15 s and again from 0.2 s to 0.25 s. The waveform clearly shows that the voltage remains unchanged from its sinusoidal nature during the dynamic changes in the load. It follows the property of insensitivity for load variations in a FOSMC. Hence the controller is said to be robust in nature.

Fig. 9 shows the tracking of output voltage for an inductive load. The load current is lagging behind the voltage by 0.8 pf. Fig. 10 displays the performance of FOSMC when VSI is fed to a non-linear load constant output voltage following the desired voltage. The instantaneous switching frequency waveform obtained shows a constant switching frequency operation at 10 KHz (Fig. 11(a,b)).Analysis of the output voltage gives the total harmonic distortion value of THD 0.135 % as shown in Fig. 12. According to IEEE 519-1992 standards lower voltage THD values less than 5 % are acceptable and hence the controller is able to deliver acceptable sinusoidal output voltage waveform.The FOSMC is able to follow the desired voltage with minimum settling time and less steady state error. To verify the insensitivity to parametric variations, the filter inductor value is changed from 1mH to 1.5 mH and the simulation is performed.
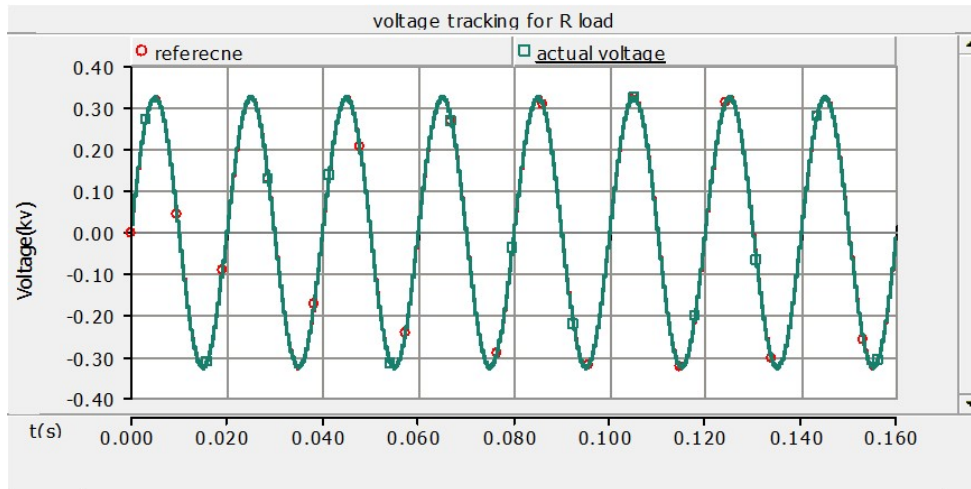
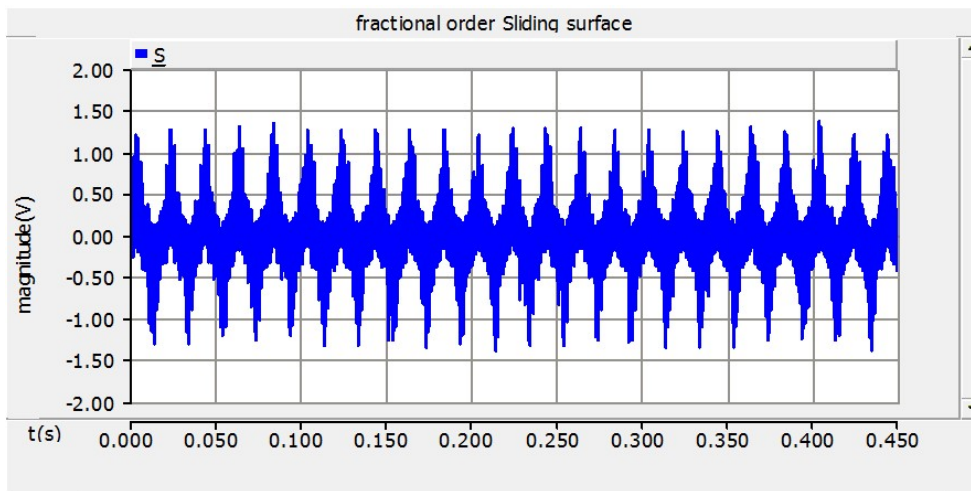*Figure 5. Tracking of reference AC voltage with the actual AC voltage.*

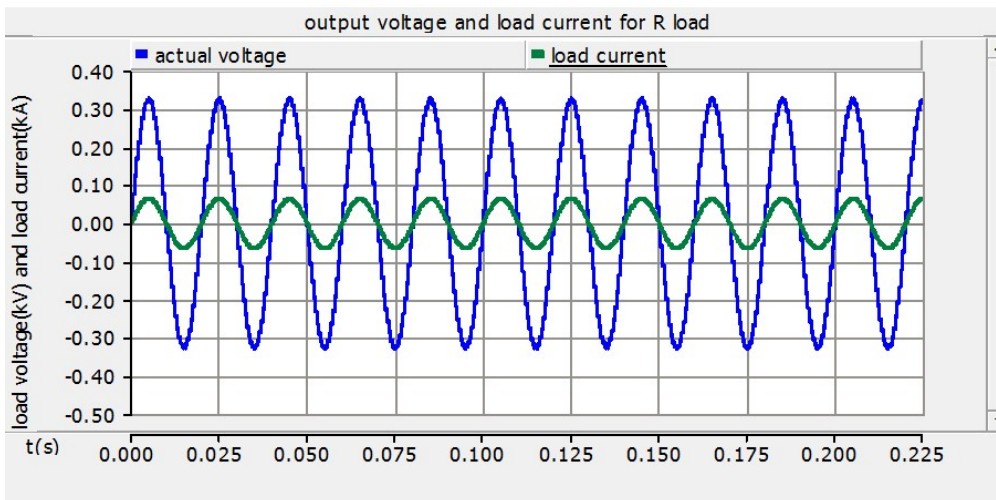*Figure 6. Fractional order sliding surface based on (4).*

Figure 7. Load current and voltage when driving a resistive load.
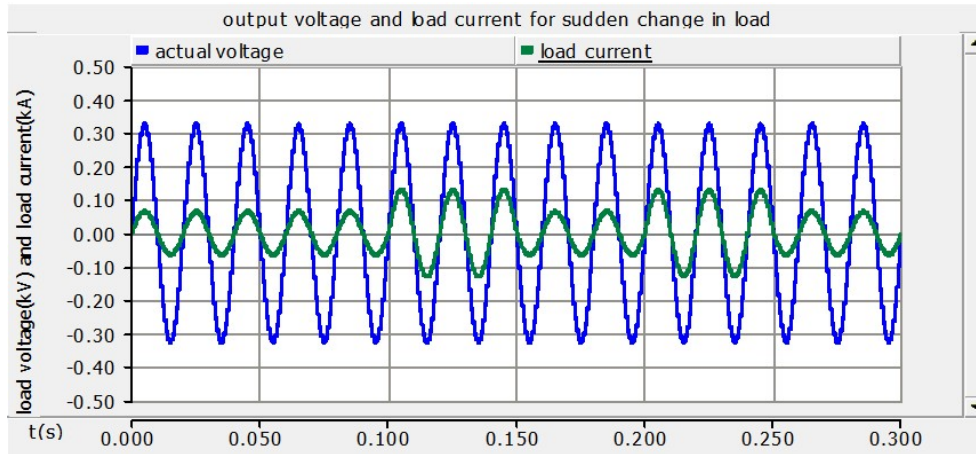
167

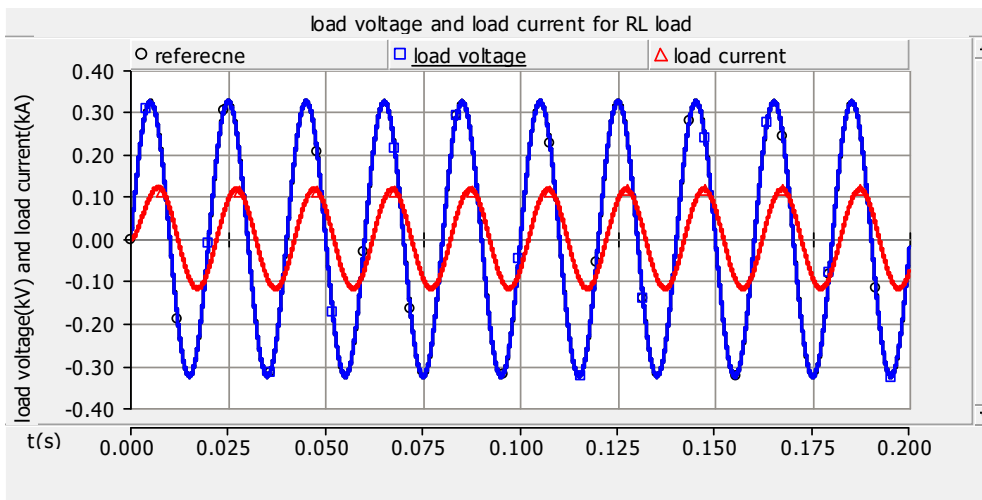*Figure 8. Dynamic response plot FOSMC.*

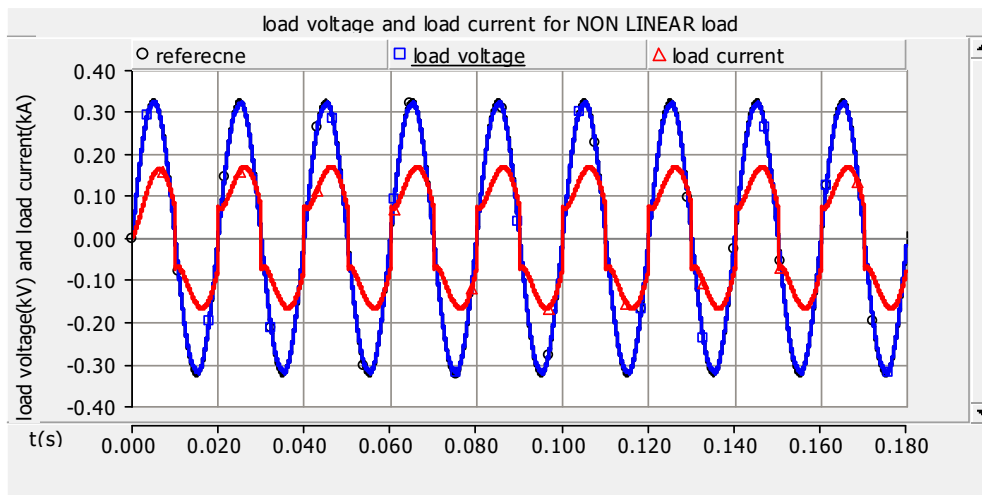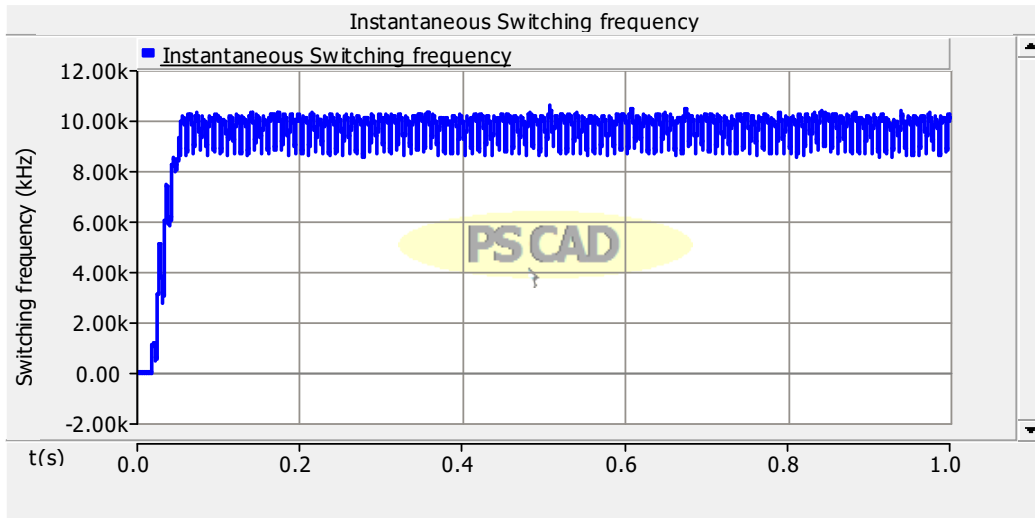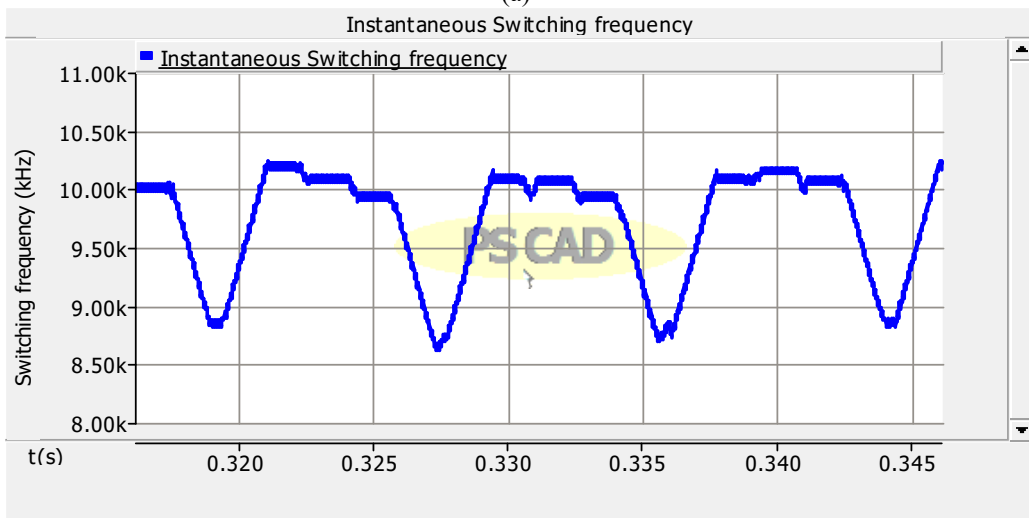*Figure 9. Voltage tracking with load current for an RL load.*

Figure 10. Output voltage tracking when non-linear load is connected.

(a)

(b)

Figure 11.(a) Instantaneous carrier frequency waveform of 10 kHz, (b) zoomed view showing maximum of 10.2 kHz and minimum of 8.7 kHz
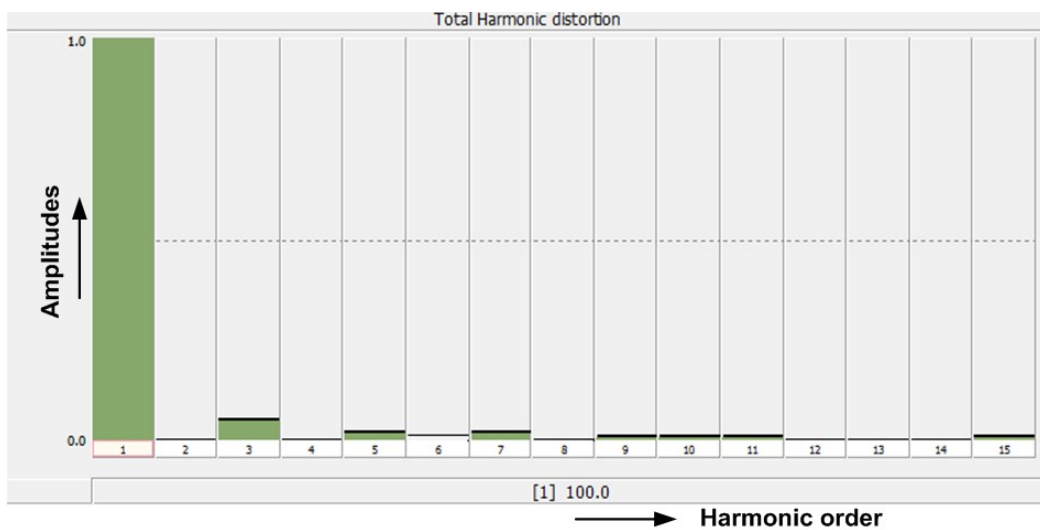

Figure 12. THD spectrum of output voltage.

Fig. 13 shows voltage across the load tracks well the reference irrespective of perturbations from 0.1s to 0.3 s. Fig. 14 shows the control efforts of SMC and FOSMC. Figs. 15 and 16 show the convergence

plotsby using the classical SMC and FOSMC, respectivelyon reaching at the origin.It is clear that the FOSMC is 8 times less in amplitude than SMC. Hence FOSMC consumes less energy and is superior in performance. FOSMC is reaching the origin in 0.37 s and requires less control energy. SMC requires 4.2 s to reach the origin.
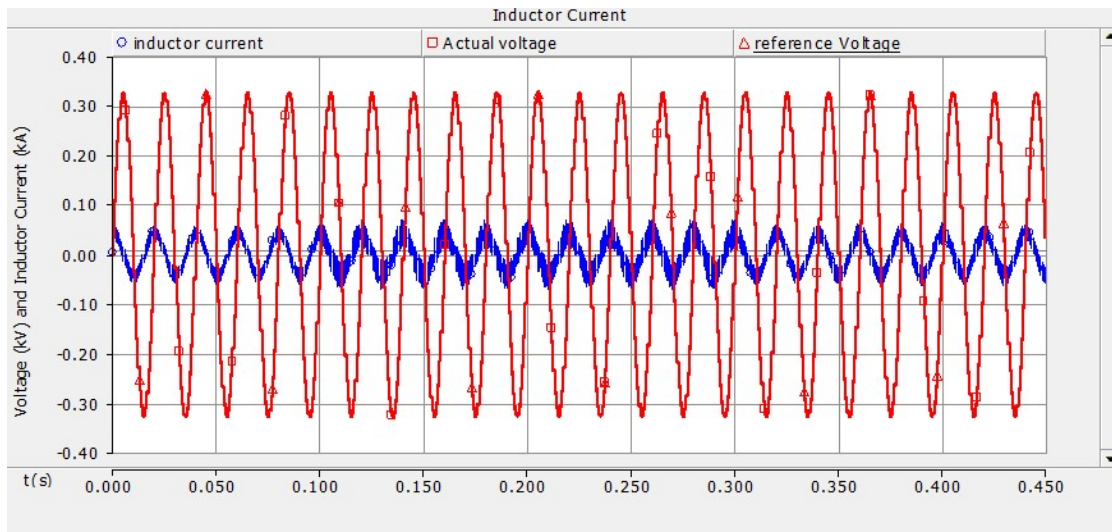

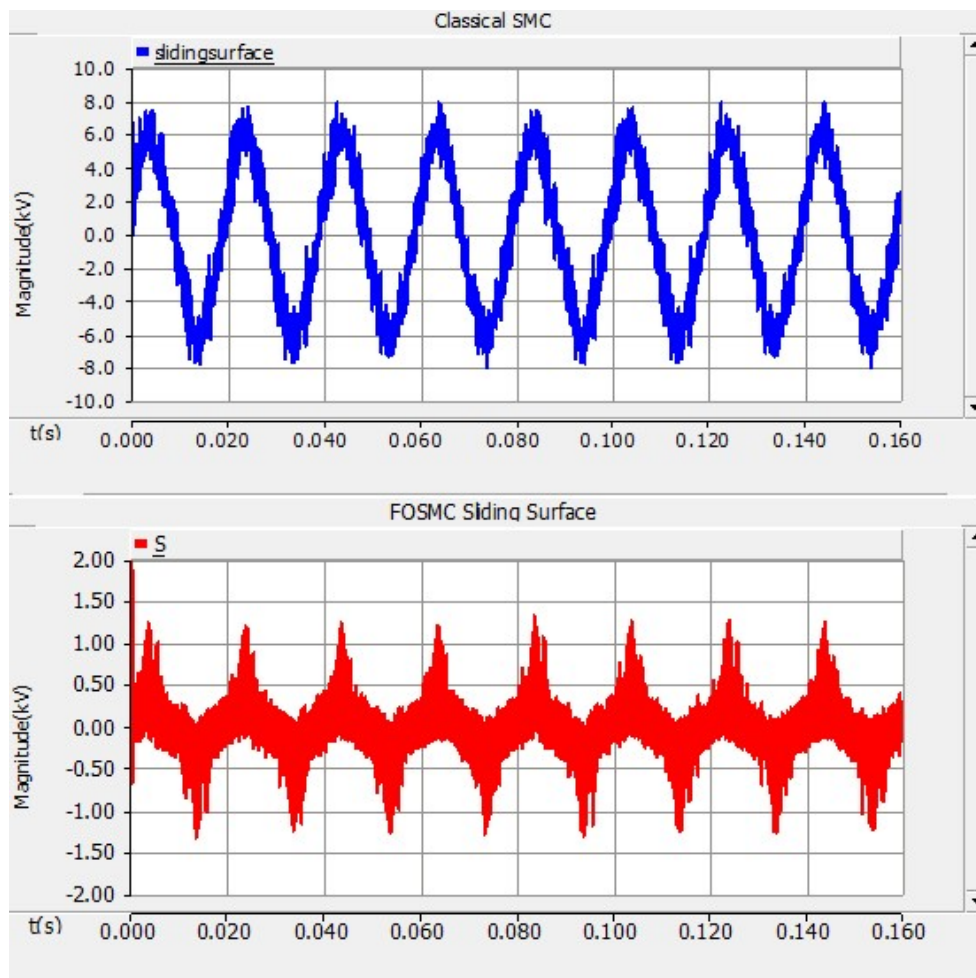*Figure 13. Tracking performance of FOSMC for filter inductor parameter variation.*
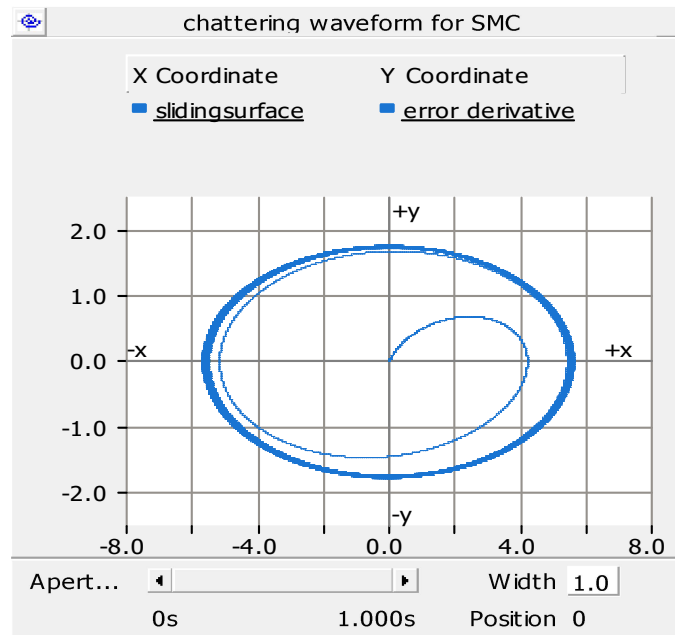

Figure 14. Sliding surface of SMC and FOSMC.

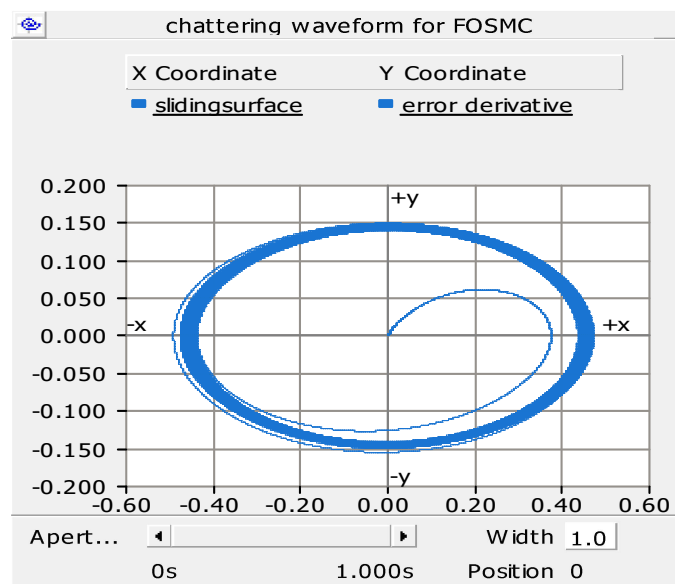*Figure 15. Convergence plot using classical SMC reaching the origin.*

Figure 16. Convergence plot using FOSMC reaching origin.

Figs. 17 and 18 shows the zoomed view of FOSMC and SMC surfaces clearly indicating the less settling time of 0.15 ms for FOSMC and 8.7 ms for SMC. Having implemented FOSMC for a VSI circuit, the authors have implemented for solar based VSI circuit which is discussed in Section 5.
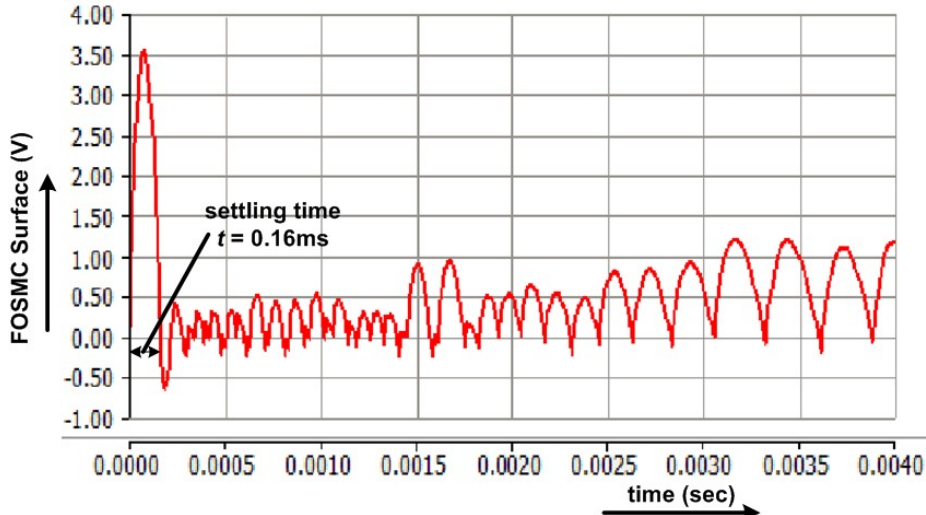
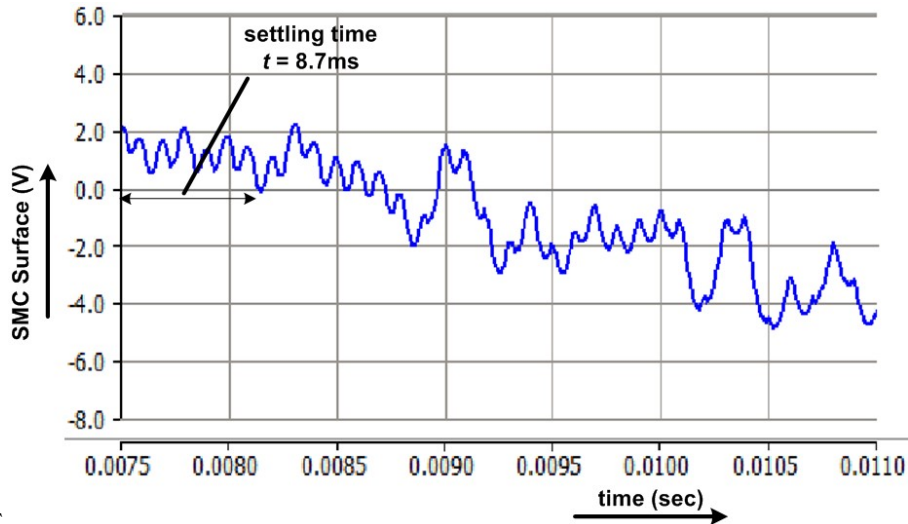*Figure 17. Amplified view of the FOSMC showing the settling time.*

Figure18. Amplified view of SMC showing the settling time.

5. SOLAR BASED DC-AC INVERTER WITH FOSMC

I-V characteristics of solar PV are widely non-linear for a PV module and have a single maximum power point.The module's highest energy output can be obtained independently of solar radiation circumstances, temperature and electrical load properties by MPPT [26]. They are Perturbing and observing (P&O), short-circuit fractional current, open-circuit fractional violation, constant voltage, neural technique and fugitive logic. There is a distinct operating point known as maximum power point (MPP) on the characteristics in which PV power is maximized. It is a simple method among the MPPT techniques [10]. It is derived from simple mathematical operations, i.e. Eqs. (19-21):

$$dp/dv = 0; V = V_{max} \qquad (19)$$

$$dp/dv = 0; V < V_{max} \qquad (20)$$

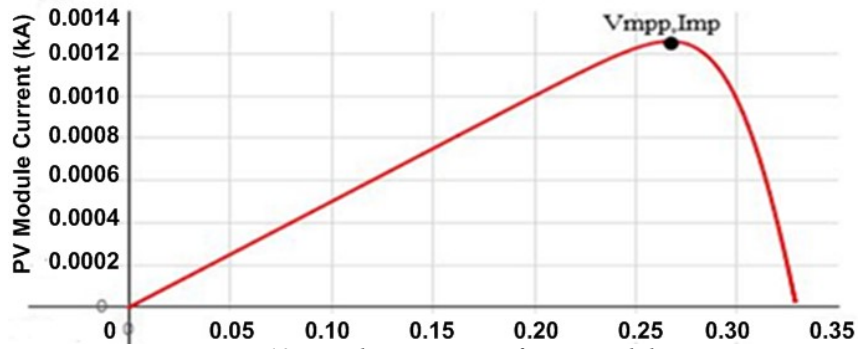$$dp/dv = 0; V > V_{max} \qquad (21)$$

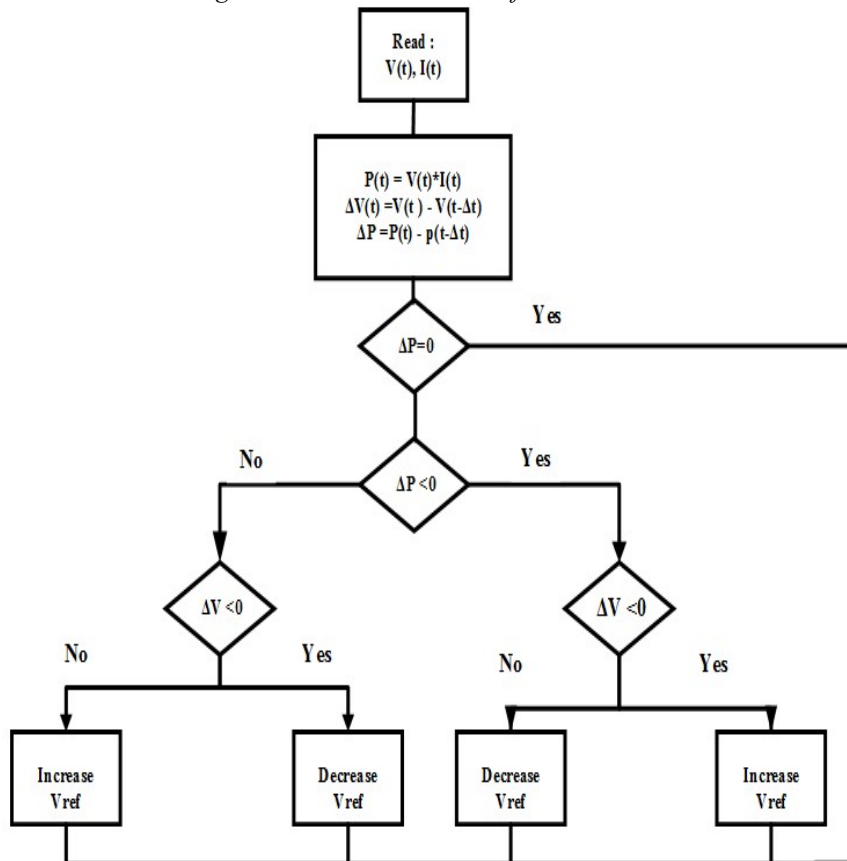*Figure19. I-V characteristic of a PV module.*

Figure20. P&O algorithm flow chart.

From Fig. 19, with increase in PV voltage, power increases during its operation on left side of the MPPT point and decreases when on right side. So for any increase in power increase, the disturbance remains unchanged to reach the MPPT. The reverse occurs for power decrease. Fig. 20 shows the flow chart of the algorithm. The instantaneous current and voltage are *I* and *V* and *ΔV* is the incremental change in voltage within a small *Δt* time period. Fig. 21(a) shows the circuit diagram for the Solar based FOSMC, while the PV characteristics is presented in Fig. 21(b,c).
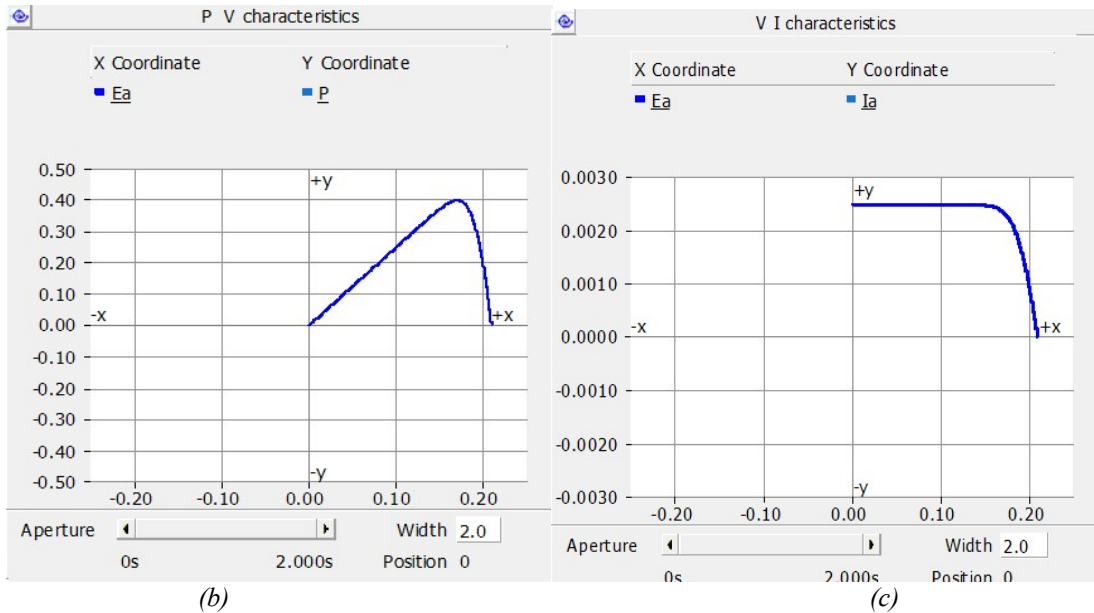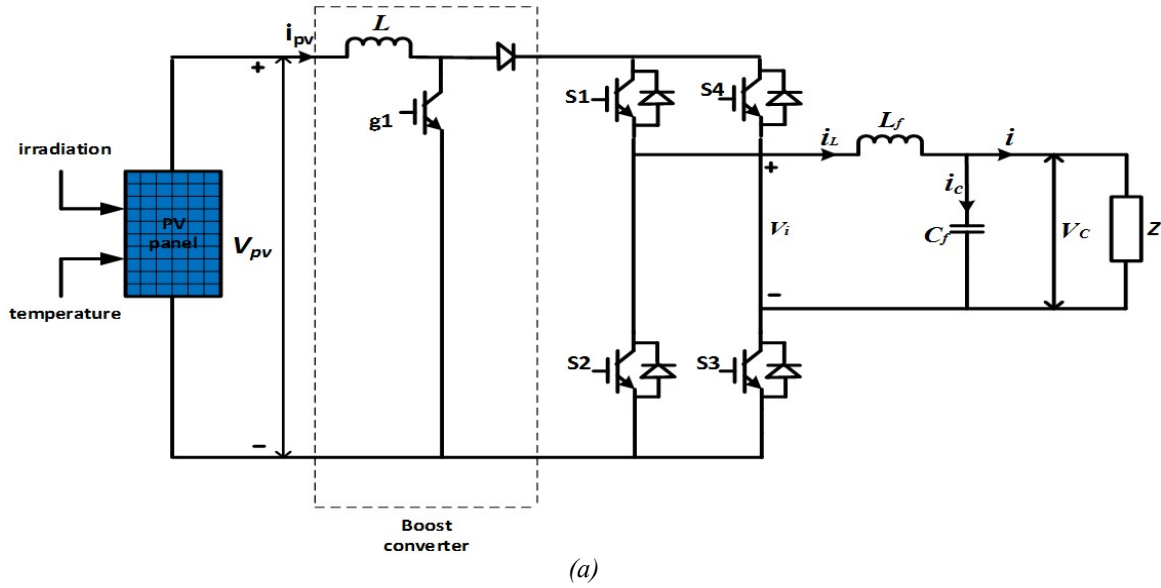
(a)

(b)   *(c)*

Figure 21. (a) Solar based FOSMC circuit diagram. PV array characteristics: (a) P-V and (b) I-V used in simulation under standard test conditions.

6. SIMULATION RESULTS AND DISCUSSIONS

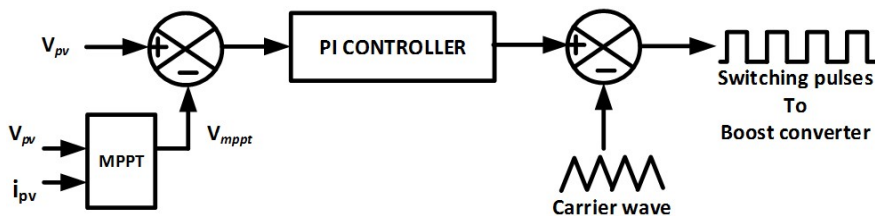Table 2 shows the PV parameters and boost converter parameters.

Fig. 22 MPPT tracking using PI controller for a Boost Converter.

Table 2 Boost Converter and PV parameters

Variables	Simulated Value
Rated PV array voltage	200 V
Inverter rating	2.5 kVA
Solar radiation, G	1000 W/m^2
Cell temperature, T	25°C
DC input voltage	400 V
Switching frequency, f_{sw}	10 kHz
Capacitor filter, C	220 μF
Inductor filter L	1.3 mH
Proportional plus Integral Controller parameters k_p and τ_i	0.5, 0.1s

The proposed Solar based DC-AC inverter with FOSMC is simulated in PSCAD v4.6. The photovoltaic array is composed of 36 cells in series to form a PV module and 29 such modules are series connected to obtain 200V. Fig. 22 shows the MPPT controller for solar PV. Fig. 23 shows the MMPT tracking of 200 V from the PV source using P&O algorithm. Figs. 24,25 show the output voltage 230V rms tracking with load current and error voltage for linear and non-linear loads. Good steady state characteristics are observed when operated with the controller. Fig. 26 shows the system converging to origin with a short settling time.
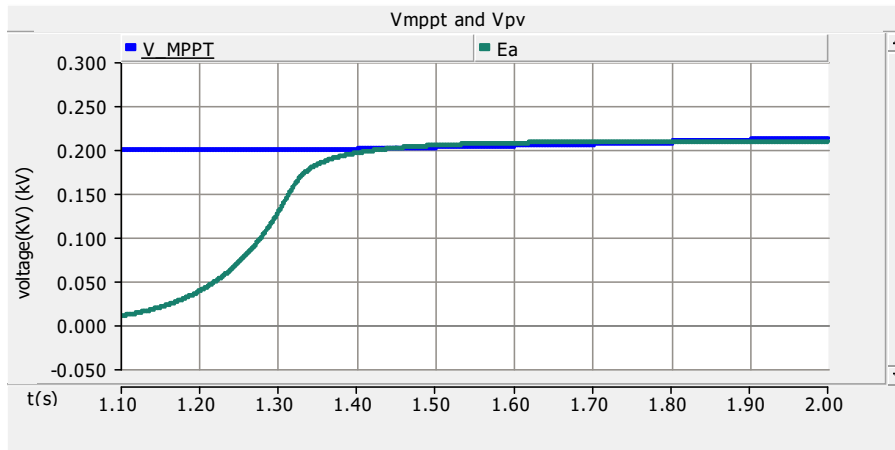

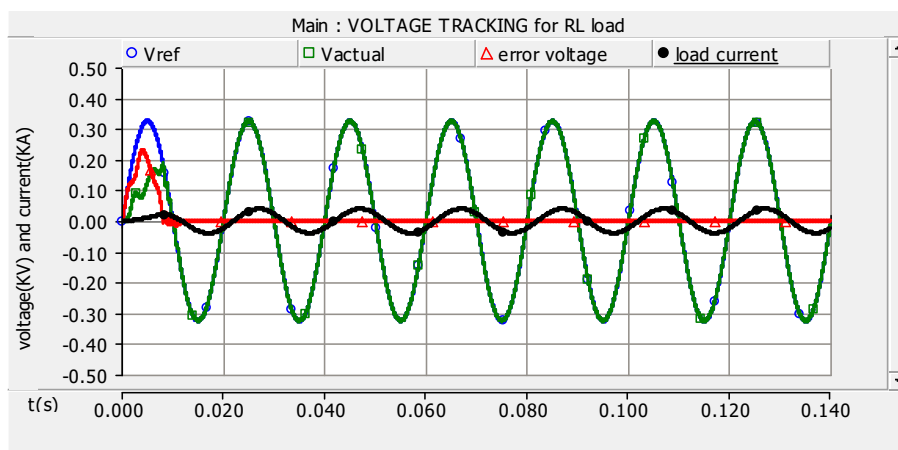*Figure 23. Tracking of MPPT voltage with PV voltage of 200V.*

Figure 24. Output voltage tracking with error voltage and load current when feeding an R_L load.
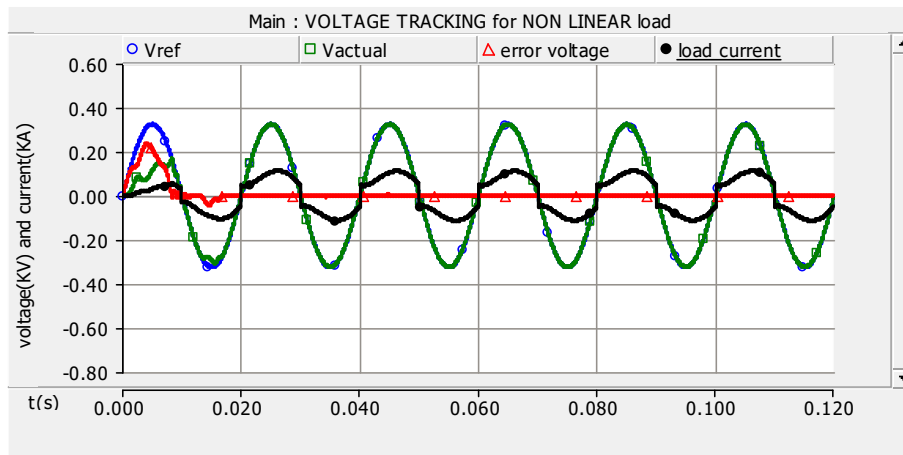
Figure 25. Output voltage tracking with error voltage and load current for a nonlinear load.
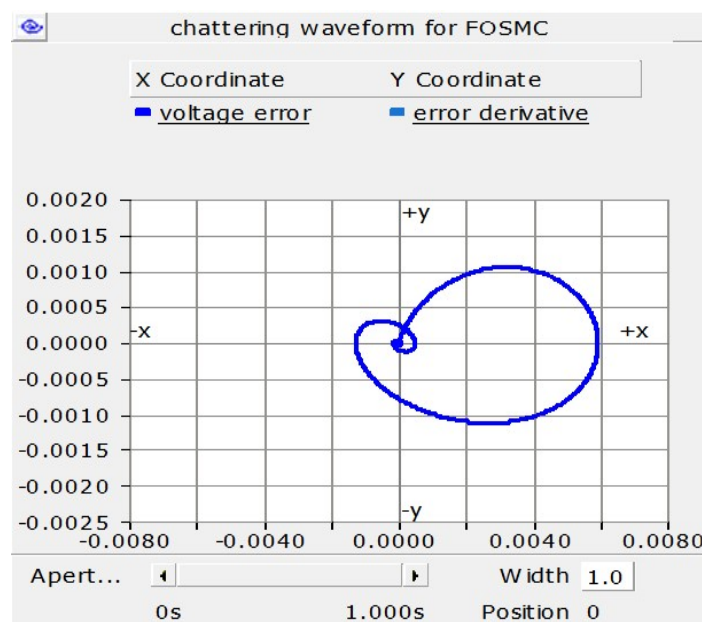

Figure 26. Phase plane plot of FOSMC of convergence.

7. CONCLUSION AND FUTURE SCOPE

The paper has designed a FOSMC control algorithm for a solar based DC-AC inverter circuit for good tracking and dynamic response of AC output voltage. It is derived from the fractional order calculus which imparts finite convergence of output AC voltage in a DC-AC inverter during steady state and when perturbed during parametric variations. By using the Lyapunov principle and using Gao's law,the FOSMC is developed. The proposed controller for DC-AC inverter is found to be better than that presented in the literature discussed in the introduction in terms of chattering, finite time convergence and steady state error with good dynamic response. Simulation results are presented for a single phase VSI to develop a sinusoidal AC voltage of 230 V (rms) as well as for Solar based DC-AC inverter circuit to realize the performance of FOSMC over the classical SMC available in the literature. For the linear and non-linear loads, FOSMC is able to generate a sinusoidal voltage with negligible error voltage for lagging as well as unity power factor loads. For a dynamic change in load within 0.2 s, the controller works well to regulate the output voltage. As compared to classical SMC, FOSMC is observed to be better in convergence, steady state error of 1.32 %, settling time of 0.15 ms, THD of 0.135 % and nearly 8 times less consumption of control energy. It is verified through phase plot, chattering is less compared to SMC. The FOSMC is found to be effective for both linear and

nonlinear type of loads in delivering a pure sinusoidal waveform of 230 V (rms) to the load. The work can be extended to a distributed generation system comprising of Solar and a battery using FOSMC. It can be used very effectively along with fast terminal SMC in higher order power electronic circuits for faster convergence.

REFERENCES

[1]Gudey,S.K., Gupta, R.,Second order sliding mode control for a single phase voltage source inverter,*TENCON 2014 IEEE Region 10 Conference;(22-25 October 2014,Bangkok, Thailand), 2014,*IEEE, 1-6, DOI: 10.1109/TENCON.2014.7022439.

[2]Delghavi, M.B., Shoja-Majidabad, S., Yazdani, A.,Fractional-order sliding-mode control of islanded distributed energy resource systems, *IEEE Transactions Sustainable Energy,2016,* 7(4), 1482-1491, DOI: 10.1109/TSTE.2016.2564105.

[3]Sudhakar, B., Satish Kumar, G.V.E.S.,Co-simulation of sliding mode control of single phase grid connected lcl filtered voltage source inverter using LabVIEW and multisim,*IEEE Region 10 Conference (TENCON)(22-25 Nov. 2016,Singapore), 2016,* IEEE, 311-315,DOI:10.1109/TENCON.2016.7848013.

[4]Marripudi, S., Gudey, S.K., Gujju, G.R.,Analysis and design of sliding mode control for MPPT based PV system with a battery storage,*14thIEEE India Council International Conference (INDICON)(15-17 December 2017,Roorkee, India),2017,* IEEE, 1-6,DOI: 10.1109/INDICON.2017.8487481.

[5]Jian, S., Zhitao, L., Hongye, S.,A second-order sliding mode control design for bidirectional DC-DC converter,*36thChinese Control Conference (CCC)(26-28 July 2017,Dalian, China), 2017,* IEEE, 9181-9186,DOI:10.23919/ChiCC.2017.8028819.

[6]Hou, B., Liu, J., Dong, F., Wang, M., Mu, A.,Sliding mode control strategy of voltage source inverter based on load current sliding mode observer,*IEEE 8thInternational Power Electronics and Motion Control Conference (IPEMC-ECCE Asia)(22-26 May 2016,Hefei, China), 2016,* IEEE, 1269-1273,DOI:10.1109/IPEMC.2016.7512471.

[7]Incremona, G.P., Rubagotti, M., Ferrara, A.,Sliding mode control of constrained nonlinear systems,*IEEE Transactions on Automatic Control,2017*, 62(6), 2965-2972,DOI:10.1109/TAC.2016.2605043.

[8]Nagaboina, V.K., Gudey, S.K.,Design and analysis of a three phase transformerless hybrid series active power filter based on sliding mode control using PQ- theory and stationary reference frames,*Serbian Journal of Electrical Engineering, 2019,*16(3), 289-310,DOI: 10.2298/SJEE1903289N.

[9]Chafekar, N., Mate, U.M., Kurode, S.R., Vyawahare, V., ADesign and implementation of fractional order sliding mode controller for DC-DC buck converter, *Fifth Indian Control Conference (ICC)(9-11 Jan. 2019,New Delhi, India), 2019,* IEEE, 201-206,DOI: 10.1109/INDIANCC.2019.8715589.

[10]Chen, Y., Petras, I., Xue, D.,Fractional order control - A tutorial,*American Control Conference(10-12 June 2009,St. Louis, MO, USA),2009,* IEEE, 1397-1411,DOI:10.1109/ACC.2009.5160719,

[11] Buchade, P.C., Vyawahare, V.A., Bhole, V.V.,Fractional-order control of voltage source inverter (VSI) using Bode's ideal transfer function,2014 International Conference on Circuits Systems, *Communication and Information Technology Applications (CSCITA)(4-5 April 2014,Mumbai, India), 2014*, IEEE, 403-407,DOI:10.1109/CSCITA.2014.6839294.

[12]Takamatsu, T., Kubo, K., Ohmori, H.,Design of fractional order sliding mode controller via non-integer order backstepping by fractional order derivative of Lyapnov function,*Proceedings of International Conference on Advanced Mechatronic Systems(10-12 Aug. 2014, Kumamoto, Japan), 2014,*IEEE, 171-174,DOI:10.1109/ICAMechS.2014.6911645.

[13] Zhu, Q., Wang, W., He, H.,Speed control system of induction motor based on fractional order control and internal model decoupling,*IEEE International Power Electronics and Application Conference and Exposition (PEAC)(4-7 Nov. 2018,Shenzhen, China), 2018,* IEEE, 1-6,DOI:10.1109/PEAC.2018.8590567.

[14]Kumar K.V.K.S.S, Rao, B.V, Kumar, G.V.E.S.,Fractional order PLL based sensorless control of PMSM with sliding mode observer,*International Conference on Power, Instrumentation, Control and Computing (PICC)(18-20 Jan. 2018, Government Engineering College, Thirussur, Kerela),2018,* IEEE, 1-6,DOI:10.1109/PICC.2018.8384774.

[15] Zeng, F., Shu, H., Zhu, T., Swe, T., Yang, B.,Fractional-order feedback linearization sliding-mode control design for grid-connected PV inverters, *IEEE 3rdInternational Electrical and Energy Conference (CIEEC)(7-9 Sept. 2019,Beijing, China), 2019,*IEEE, 874-878,DOI: 10.1109/CIEEC47146.2019.CIEEC-2019334.

[16] Calderon, A, J.,B.,M., Vinagre and Feliu, V., Fractional Sliding Mode Controlof a DC-DC Buck Converter with Application to DC Motor Drives, *ICAR 2003, The 11th Inter. Conf. on Advanced Robotics, Coimbra, Portugal, 2003,* IEEE, 252-257.

[17] Ningning, Y., Chaojun, W., Rong, J., &Chongxin L., Fractional-Order Terminal Sliding-Mode Control for Buck DC/DC Converter. *Mathematical Problems in Engineering, 2016,* Hindawi, 1-7, DOI: 10.1155/2016/6935081.

[18] Wang, J., Xu, D., Zhou, H., Bai, A., Lu, W., High-performance fractional order terminal sliding mode control strategy for DC-DC Buck converter, *PLoS ONE, 2017,* 12(10), e0187152. DOI: 10.1371/journal.pone.0187152.

[19] Mudaliyar, S., R., Pullaguram, D., Mishra, S., Senroy, N. Cascaded Fractional Order and Sliding Mode Control for an Autonomous Voltage Source Inverter, *2018 IEEE Power & Energy Society General Meeting (PESGM), Portland, OR, 2018,* IEEE, 1-5, DOI: 10.1109/PESGM.2018.8585985.

[20] Pan, M., Chen, C., Zhang, D. Fractional-order Sliding Mode Control Strategy for Quasi-Z Source Photovoltaic Grid-Connected Inverter, *2019 IEEE 3rdConference on Energy Internet and Energy System Integration (EI2), Changsha, China, 2019,* IEEE, 939-943, DOI: 10.1109/EI247390.2019.9061871.

[21] Kumar, V., Ali, I.,Fractional order sliding mode approach for chattering free direct power control of DC/AC converter,*IET Power Electronics, 2019,*12(13), 3600-3610, DOI: 10.1049/iet-pel.2018.5662.

[22]Babes, B., Boutaghane, A., Hamouda, N., Mezaache, M.,Design of a robust voltage controller for a DC-DC buck converter using fractional-order terminal sliding mode control strategy, *International Conference on Advanced Electrical Engineering (ICAEE)(19-21 Nov. 2019, Algiers, Algeria), 2019,*IEEE, 1-6, DOI: 10.1109/ICAEE47123.2019.9014788.

[23]Xing Z., Hong Z., Fei L., Fang L., Chun L., Benxuan L., An LCL-LC power filter for grid-tied inverter,TENCON *IEEE Region 10 Conference,(22-25 Oct. 2013,Xi'an, China), 2013,* IEEE, 1-4,DOI:10.1109/TENCON.2013.6718873.

[24]Ang, Y., Bingham, C., Foster, M., Howe, D., Design oriented analysis of fourth-order LCLC converters with capacitive output filter,*IEEE Proceedings -Electric Power Applications, 2005,*152(2),IEEE, 310–322, DOI: 10.1049/ip-epa:20045112.

[25]Olalla, C., Clement, D., Rodriguez, M., Maksimovic, D., Architectures and control of submodule integrated DC–DC converters for photovoltaic applications, *IEEE Trans. Power Electronics, 2013*, 28(6), 2980–2997, DOI: 10.1109/TPEL.2012.2219073.

[26]Adak, S., Cangi, H., Yilmaz, A., Design of an LLCL type filter for stand-alone PV systems' harmonics, *Journal of Energy Systems, 2019*, 3(1), 36-50, DOI: 10.30521/jes.506076.